Prediction of Treatment Outcome to Transcranial Direct Current Stimulation in Major Depression Based on Deep Learning of EEG Data

Jijomon Chettuthara Moncy
School of Psychology
University of East London
London, United Kingdom
ORCID 0000-0002-5628-7827

Yong Fan
Department of Radiology,
Perelman School of Medicine
University of Pennsylvania
Philadelphia, United States of America
ORCID 0000-0001-9869-4685

Cynthia H.Y. Fu
School of Psychology,
University of East London
Centre for Affective Disorders, IoPPN,
King's College London
London, United Kingdom
ORCID 0000-0003-4313-3500

***Abstract*—Major Depressive Disorder (MDD) is a leading cause of disability worldwide. Current first line treatments are antidepressant medication and psychotherapy. However, they have limited effectiveness and there are no biomarkers that can predict treatment response at the individual level. Transcranial direct current stimulation (tDCS) is non-invasive brain stimulation method that is a potential novel treatment for MDD. The present study sought to investigate neural biomarkers for predicting response to tDCS at the individual level using portable EEG. The clinical trial was a double-blinded, placebo-controlled, randomized, superiority trial of home-based tDCS. Participants were randomized to a 10-week course of either active or sham tDCS sessions. Resting state, eyes closed EEG data were acquired at baseline, prior to starting tDCS, and at week 10. EEG data acquisition was conducted using a portable, 4-electrode EEG device (Muse). The baseline EEG data from 21 participants were used to train and test the deep learning models of 1D convolutional neural networks (1DCNNs), Long Short-Term Memory (LSTM), Gated recurrent units (GRU) and the hybrid models combining 1DCNN and LSTM/GRU. A prediction rule was proposed and applied to the classifier outputs of each participant and the treatment outcomes were predicted. Different combinations of power spectral density vectors extracted from the EEG frequency bands of four electrodes were selected to improve the treatment outcome prediction. Using 1DCNN model the work achieved a treatment outcome prediction accuracy 85.7%, with a specificity of 71.4% for predicting treatment remission and sensitivity of 92.8% for predicting residual depressive symptoms, which was based on the combined theta and alpha EEG band power spectral density from the TP10 electrode.**

Keywords— deep learning, major depression, MDD, treatment outcome, CNN, LSTM, GRU, treatment remission, transcranial direct current stimulation

I. Introduction

Major depressive disorder (MDD) represents a significantly prevalent and debilitating mental health disorder, characterized by persistent feelings of a low mood or inability to experience pleasure that is associated with a diminished interest in daily activities and changes in neurovegetative symptoms [1]. It stands as one of the leading contributors to global disability [2], with a lifetime prevalence estimated at 17% [3], thereby constituting a substantial economic burden [4]. Treatment of MDD remains challenging, related to the heterogeneity of the disorder and limited effectiveness of current treatment options [5]. Furthermore, treatments require several weeks duration to evaluate efficacy [6]. In recent years, research has focused on identifying neurological biomarkers of treatment response from electroencephalogram (EEG) data. EEG, being portable, offering high temporal resolution, and is cost-effective, emerging as a potential tool for such investigations. It enables the observation of neurological changes in the brain and has shown promising results in detecting treatment outcomes in MDD [7]. Pre-treatment differences in theta band resting activity in the rostral anterior cingulate cortex were observed between responders and non-responders to antidepressant treatment [8]. Increased anterior cingulate cortex activity is reported as a reliable biomarker for antidepressant treatment response [9]. EEG signals from 21 electrodes during eyes closed resting state prior to treatment in 52 MDD participants showed that improvements in depressive severity were negatively related to delta and theta wave activity and positively related to beta activity at frontal recording sites [10]. Moreover, increased frontocentral theta EEG power, a slower anterior individual alpha peak frequency, a larger P300 amplitude, and decreased pre-frontal delta and beta cordance were predictors of non-response to repetitive transcranial magnetic stimulation (rTMS) [11].

Recent advancements in machine learning and deep learning techniques have revolutionized treatment outcome prediction. One of the key strengths of machine learning systems lies in their adaptability and ability to be trained based on provided data. The Establishing Moderators and Biosignatures of Antidepressant Response in Clinical Care (EMBARC) study [12], which consisted of 309 MDD participants in a placebo-controlled antidepressant study, introduced Sparse EEG Latent SpacE Regression (SELSER), a machine learning algorithm predicted treatment outcomes using band powers by encompassing spatial filtering, band power feature extraction, and linear regression [13]. Pre-treatment resting-state EEG data was used to train the algorithm. To validate the method's efficacy, it was tested on three additional datasets containing signals from 60 or more electrodes. The treatment outcome was quantified by measuring the pre-minus-post treatment differences in Hamilton Rating Scale for Depression (HAMD) [14] scores. Alpha waves from the resting eyes open condition significantly predicted the observed treatment score changes, particularly for sertraline efficacy prediction [13]. Numerous studies have examined the classification or prediction efficacies in assessing the treatment response across various MDD treatments from EEG signals. A random forest classifier utilizing features from EEG data collected by 32 electrodes achieved a 78% accuracy in predicting antidepressant response [15].

CHYF acknowledges grant support from the Rosetrees Trust (CF20212104), Flow Neuroscience.

979-8-3503-5409-6/24/$31.00 ©2024 IEEE
DOI 10.1109/CAI59869.2024.00201

TABLE I. DEMOGRAPHIC AND CLINICAL CHARACTERISTICS OF TOTAL PATIENTS AT BASELINE

Characteristic	Active Treatment	Sham Treatment
Number (Female)	12 (9)	9 (9)
Age (years)	38.00 ± 9.31	35.88 ±10.64
Age of onset (years)	18.00 ± 6.07	25.00 ± 9.81
Previous number of episodes	2.9 ± 3.1	5.4 ± 7.6
In first episode MDD	3	2
Clinical ratings		
HAMD	18.91±1.83	17.88±1.53
MADRS[a]	25.33±3.86	21.88±2.93
Taking antidepressant medication	7	5
In individual psychotherapy	0	1
No other treatment during trial	5	4

[a.] A significant difference between groups was found for MADRS score, p = 0.038. There were no significant differences for any other characteristics.

Using EEG signals from 16 electrodes selective serotonin reuptake inhibitor (SSRI) treatment response is correctly predicted with an accuracy of 87.9% in [16].

Treatment outcome prediction for tDCS using baseline EEG and the combination of Support Vector Machine (SVM), Linear Discriminant Analysis (LDA), and Extreme Learning Machines (ELM) classifiers, treatment response in mood and cognition is predicted with accuracies of 71 ± 11% (Tp9) and 87 ± 5% (Pz), respectively, [17]. Pretrained convolutional neural network models through transfer learning achieved a 96.55% accuracy in classifying responders and non-responders to SSRI antidepressant treatment in [18]. For predicting rTMS treatment outcomes, [19] reported a mean accuracy of 92.28%.

All these studies conducted EEG signal acquisition in controlled laboratory environments with multielectrode systems, requiring significant time and effort for head preparation. In our study, we introduced a novel approach of home-based tDCS treatment for MDD [20, 21]. In addition, participants conducted EEG acquisition at their own home with real-time guidance from researchers through video calls, using a portable wireless 4-dry electrode EEG device. The power spectral density (PSD) estimated from the baseline/pre-treatment EEG signals from 4 electrodes were used as inputs to the different deep learning architectures. Electrode selection and EEG band selections were performed to improve the deep learning model's classification accuracy. We have also proposed a prediction rule to make use of the entire EEG signal. We have evaluated the treatment response prediction accuracy using a leave-one-subject-out manner. Despite the constraints due to remote home based data collection and limited number of electrodes, our study achieved a comparable treatment outcome prediction accuracy to other investigations.

II. PARTICIPANT RECRUITMENT AND EEG DATA COLLECTION

All participants provided written informed consent for participation. Ethical approval was provided by South Central-Hampshire B Research Ethics Committee UK. EEG data were acquired from a subsample of 21 MDD participants (18 women), with a mean of 37.1 years in age, standard deviation of 9.7 years. Clinical and demographic data of all participants in the study can be found in [21]. Inclusion criteria included being aged 18 years or older, a diagnosis of unipolar MDD with a current depressive episode as defined by the diagnostic criteria in the Diagnostic and statistical manual of mental disorders – 5th edition (DSM-V) [1], with a HAMD of $\geqslant$ 16, determined by a structured assessment using the Mini-International Neuropsychiatric Interview (MINI; Version 7.0.2) [22]. All participants being medication-free for 6 weeks prior to enrolment or taking a stable antidepressant medication with a stable medication source and agreeing to continue the same regimen throughout study participation, or if in psychotherapy, have maintained stable psychotherapy for at least 6 weeks prior to enrolment. Exclusion criteria included having a history of mania or psychosis, having treatment resistant depression, having a neurological disorder or a medical disorder that may mimic mood disorders, a history of hospital admission for depression or suicidal behaviour, or any exclusion criteria for receiving tDCS. Participants were recruited from online advertisements and general practitioner (GP) referrals.

Fig. 1. MUSE EEG recording device.

The study was a double-blind, placebo-controlled, randomized, superiority, remote trial. During the treatment phase, participants were randomized into one of the two arms: active and sham tDCS for 10 weeks. The participants were divided equally between the arms and were not informed of their assignment. The active or sham tDCS sessions were self-administered by participants in their homes 5 times a week for 3 weeks and then 3 times a week for 7 weeks, for a total of 36 sessions. After the completion of the blinded treatment phase all participants were offered to continue the treatment. Participants in the sham group were offered the active tDCS and participants in the active group were offered to continue maintenance treatment. Among the 21 MDD participants, 12 had been randomised to the active tDCS treatment arm, and 9 had been randomised to the sham treatment group.

Each participant received real-time guidance by videoconference by trained research team members. Four 5-minute pre-treatment EEG sessions recordings were made for each participant at their home. During EEG data collection, participants were instructed to sit relaxed without making any body movements. Two of the 5-minute recordings were performed with the participants' eyes closed, and two were conducted during a resting state with eyes open. EEG recordings were obtained using a 4-electrode Muse device shown in Fig. 1., with a sampling frequency of 256 Hz. EEG data acquisition was performed using a wireless, low-cost, and easy-to-wear device equipped with four dry electrodes. The frontal electrode positions were AF7 and AF8, while the temporoparietal electrode positions were TP9 and TP10. The EEG signals were referenced to the FPz electrode. The recorded EEG signals were saved in CSV format, containing timestamps for each EEG sample, raw EEG signals from each electrode, Horse Shoe Indicator (HSI) values for each electrode, and other relevant information. The HSI values indicate the quality of electrode connectivity.

III. EEG SIGNAL PRE-PROCESSING

Treatment remission was defined as HAMD score at week 10 being less than 8. Participants were divided into two groups: remission and non-remission to tDCS treatment based

on their HAMD rating at the end of the RCT at 10 weeks. In the active treatment arm, 6 participants achieved remission and 6 participants non-remission. In the sham treatment arm, 1 participants attained remission and 8 participants non-remission.

For the deep learning based classification of MDD remission versus non-remission, two 5-minute-long EEG recordings during eyes closed state were utilized. Each of these recordings was divided into 60 non-overlapping EEG windows, each spanning 10 seconds. Each EEG sample from all electrodes was associated with an HSI value, indicating electrode connectivity quality. A value of 1 represented good connectivity, 2 denoted average connectivity, and 4 indicated poor connectivity. To further process the EEG windows, the HSI values were averaged over the samples, and windows with an average HSI below 2 were selected.

For each participant in both groups, PSD is estimated from the selected EEG windows. Given the resting-state eyes closed paradigm during EEG data collection, where time-locked evoked potentials were not expected, we focused on extracting relevant information in the frequency domain rather than the time domain. Each windowed EEG segment was transformed into its corresponding PSD vectors using Welch's periodogram method [23]. To estimate the PSD using Welch's method, the 10-second EEG windows were further divided into 3-second sub-windows with a 2-second overlap. The resulting PSD contained half the number of frequency points compared to the time domain EEG samples in each window. Considering a sampling frequency of 256 Hz, the maximum frequency content in the PSD was 128 Hz. The DC component, representing the 0 Hz frequency component in the PSD, is constrained to zero to eliminate the impact of baseline shifts in the EEG signals. In training the deep learning models, power density values associated with different frequency bands were extracted from the estimated PSD and employed as input vectors.

IV. Deep Learning Model and Prediction Rule

To predict the treatment outcome of a given participant regarding remission status, we employed deep learning models using different architectures including one-dimensional convolutional neural networks (1DCNNs), Long Short-Term Memory (LSTM) networks, Gated recurrent units (GRU) networks and the hybrid models combining 1DCNN and LSTM/GRU architectures. Recurrent Neural Networks (RNNs) represent a pivotal class of neural networks tailored for sequential data processing. They are designed to retain information from preceding inputs and excel in scenarios where temporal dependencies matter. Since we provide power spectral density vectors as inputs to the neural networks, the dependencies between frequencies will be evaluated by RNNs. Within the realm of RNNs, Long Short-Term Memory (LSTM) networks [24] and Gated Recurrent Units (GRUs) [25] emerge as prominent architectures. The designs of LSTM and GRU specifically target the challenge of "vanishing gradients" encountered in conventional RNNs. Vanishing gradients pose a significant hurdle, arising when the gradients of the network weights diminish to an extent that impedes effective learning. By incorporating memory cells and strategically placed gates, LSTMs and GRUs empower the network to selectively store and retrieve information, facilitating more effective learning and capturing of frequency patterns in the PSD inputs. Whereas convolutional neural networks were designed to exploit patterns' invariance within

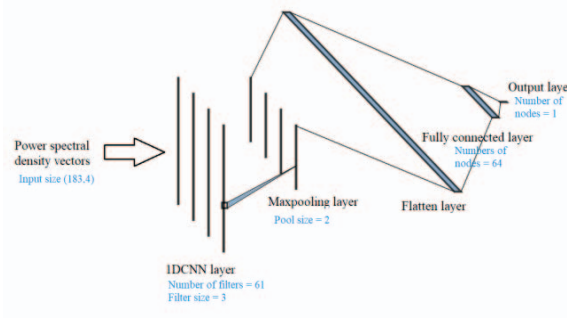

Fig. 2. 1DCNN deep learning architecture for the full-band PSD input of 4 electrodes.

a given domain [26]. In image processing, spatial invariance refers to the invariance of 2-dimensional shapes, while in the context of one-dimensional signals such as EEG data or power spectral density, it can represent signal-specific patterns like an event-related potential (ERP) or a peak within a frequency band. In this work 1DCNNs gave highest classification accuracy and prediction accuracy compared to other architectures. The details of the classification accuracies are given in the results and discussion section.

The 1DCNNs employ one-dimensional convolutional filters, which slide along the input sequence, capturing local dependencies and hierarchies. Non-linear activation functions typically follow the convolutional operation, introducing non-linearity to the model. Pooling layers can be utilized to reduce dimensionality and down sample the feature representations, thereby facilitating efficient feature learning. The learned features are then fed into fully connected layers, empowering the network to learn complex relationships and make predictions.

The number of filters used in the initial layer of the deep learning model was adjusted based on the input vector dimension. For single electrode EEG, the PSD vector, representing all EEG bands (0-60 Hz) including delta (0.5-4 Hz), theta (4-8 Hz), alpha (8-12 Hz), beta (12-30 Hz), and gamma (30-60 Hz), had a dimension of 183. In this case, we utilized 27 filters with a kernel size of 3 for 1DCNN models. However, when focusing solely on the alpha band, we employed only 5 convolutional filters with a kernel size of 3. Similarly, when classifying PSD with all EEG bands from all 4 electrodes, the input vector size was 183x4, while for a single electrode classification, it was 183x1. In the utilization of LSTM and GRU architectures, the number of LSTM/GRU units was adjusted based on the dimension of the input vectors. For instance, when dealing with the alpha band PSD having a dimension of 12x4, we employed 4 LSTM/GRU units for modelling the network. A visual representation of the 1DCNN model used to classify the PSD input vector containing full EEG bands (0-60 Hz) and 4 electrodes can be found in Fig. 2.

To assess the effectiveness of deep learning models for remission vs. non-remission participant classification, we conducted subject independent, leave-one-subject-out (LOSO) testing. Out of the 21 participants, one was excluded for testing, and from the remaining 20 participants, four (two from each class) were used for validation, leaving the data of 16 participants for training the model. Considering 10 minutes of EEG signals for each participant, the estimated PSD vectors contributed by each participant were 60, although the actual

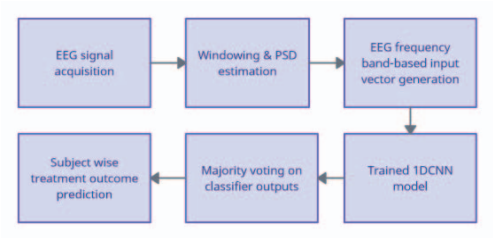

Fig. 3. EEG based treatment outcome prediction scheme.

count might be slightly lower due to the omission of certain EEG windows with HSI values greater than 2. In total, there were 1235 PSD vectors available from all participants, resulting in an average of 58.81 training samples per participant. The deep learning model training was halted after 50 epochs, and the model with the highest validation accuracy was selected for testing. This process was repeated for every participant, and their corresponding testing accuracies were recorded.

We employed a prediction rule, commonly used in multi-instance learning, to determine the treatment outcome based on the collective classifier outputs for each participant. The assignment of a participant to a specific treatment outcome depended on the majority class prediction among its samples. In essence, a participant was assigned to a class only if more than 50% of its samples were classified into that class. Complete treatment outcome prediction scheme is depicted in Fig. 3. For instance, consider a specific participant (ID 21), , where 55% of its samples (PSD vectors) were classified into the remission class and 45% into the non-remission class. Applying this rule led to the prediction of treatment remission. This prediction rule makes use of the entire 10-minute EEG signals to predict the treatment outcome.

V. Results and Discussion

Incorporating PSDs from all four electrodes, covering the full EEG frequency bands from 0 - 60 Hz, and trained the deep learning model, the average classification accuracy obtained for the different deep learning models were between 50% to 60%. Further we trained different deep learning models using PSD vectors from all four electrodes for the individual EEG bands, i.e., delta, theta, alpha, beta, and gamma bands and the corresponding average classification accuracies are presented in Table II. Considering the individual band PSD vectors as inputs for classification, the highest classification accuracy is obtained for alpha band. The CNN, GRU and combined CNN, GRU architectures obtained classification accuracies of 64.62%, 64.87%, and 64.18% respectively. It is essential to highlight that these average classification accuracy rates, as shown in Table II, represents averaged performances of each of the deep learning models in LOSO testing before applying the treatment outcome prediction scheme. Notably, the classification accuracy rates for the alpha and gamma bands were significantly higher compared to the other frequency bands.

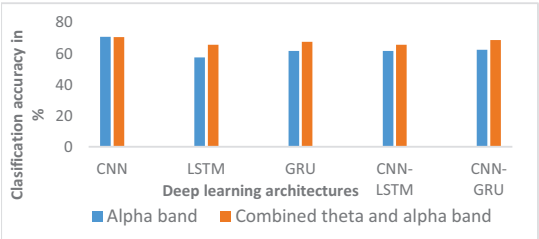

Fig. 4. Classification accuracies obtained for different deep learning architectures for the band selected PSD vectors from TP10 electrode.

We systematically investigated combinations of EEG bands. To achieve this, we experimented with all possible combinations of 2, 3, and 4 EEG bands extracted from the four electrodes. These combinations were then utilized as inputs to the model, and the resulting classification accuracies were examined. We noted enhanced classification accuracies when combining different frequency bands, showcasing the effectiveness of diverse EEG band combinations. To delve deeper into the analyses, we explored the individual contribution of each electrode in achieving these high classification accuracies using the bands that surpassed 60% accuracy for 1DCNN model with all four electrodes. By independently employing PSDs from each electrode for classification, we examined the performance. The PSD from the alpha band and the combination of theta and alpha bands from the TP10 electrode yielded the highest classification accuracies, reaching above 70%. Fig. 4. illustrates the classification accuracies achieved by various deep learning architectures using PSD vectors from the alpha band and the combination of theta and alpha bands from the TP10 electrode. To investigate the influence of frontal and temporoparietal hemispherical asymmetry on classification, we individually trained the model using PSDs from AF7, AF8 and TP9, TP10 electrode pairs, specifically for the bands and band combinations that achieved more than 60% accuracy using all four electrodes. Notably, the TP9, TP10 pair from the theta-alpha band combination and the alpha-beta band combination achieved classification accuracies close to 70.34%. From all the band combinations and electrode selections, the highest classification accuracies were obtained as 70.62% and 70.52% for the 1DCNN with PSD vector inputs from alpha band and the combined theta and alpha bands respectively. With accuracies around 70% from using only the TP10 electrode with the alpha band and the combination of theta and alpha bands, we proceeded with these configurations to predict treatment remission.

We selected the bands and band combinations that attained classification accuracies close to 70% and applied the prediction rule to each participant's classification accuracy. The participant-wise classification accuracies of the selected bands and band combinations are provided in Table III. Specifically, for participant 11, using alpha band PSD from the TP10 electrode resulted in a 37% classification accuracy, implying that only 37% of the total input PSD vectors were correctly classified into the non-remission class.

TABLE II. Deep learning architecture-wise classification accuracy for different frequency band input vectors from 4 electrodes

Frequency bands	Classification Accuracies for different architectures in %				
	CNN	***LSTM***	***GRU***	***CNN & LSTM***	***CNN & GRU***
Delta	53.76	54.68	59.84	54.75	58.51
Theta	55.76	53.44	56.92	51.07	55.25
Alpha	64.62	60.06	64.87	59.54	64.18
Beta	54.43	57.35	55.84	55.65	53.89
Gamma	63.14	56.76	54.63	61.32	59.26

TABLE III. PARTICIPANT-WISE CLASSIFICATION ACCURACY FOR THE ALPHA BAND AND THE COMBINATION OF THETA AND ALPHA BANDS FROM TP10 ELECTRODE

Participant ID	Active/ Sham	Treatment outcome	Rounded classification accuracies in %	
			Alpha band	*Theta and Alpha bands*
01	Sham	Non-remission	95	96
02	Sham	Non-remission	90	82
03	Active	Non-remission	90	91
04	Sham	Non-remission	68	68
05	Sham	Non-remission	69	98
06	Sham	Non-remission	86	70
07	Sham	Non-remission	93	96
08	Active	Non-remission	90	87
09	Active	Non-remission	98	95
10	Sham	Non-remission	96	98
11	Active	Non-remission	37	8
12	Active	Remission	0	10
13	Active	Non-remission	96	82
14	Active	Remission	0	0
15	Active	Non-remission	81	95
16	Active	Remission	54	62
17	Sham	Non-remission	83	89
18	Active	Remission	50	56
19	Active	Remission	96	91
20	Sham	Remission	41	52
21	Active	Remission	70	55

Similarly, the combined theta and alpha band PSD from the TP10 electrode achieved a classification accuracy of only 8%. For treatment remission, using alpha band PSD from the TP10 electrode, four out of seven participants had a classification accuracy lower than or equal to 50%. Conversely, only 2 participants had a classification accuracy lower than or equal to 50% for PSD vectors in the combined theta and alpha bands from TP10.

In the present study, we defined the positive class as the non-remission group. We applied the prediction rule to the classification accuracies obtained from the alpha band and the theta-alpha band combination. Using the alpha band in conjunction with the TP10 electrode, we correctly predicted the treatment outcomes for 16 out of 21 participants, yielding a prediction accuracy of 76.19%. However, employing the combined theta and alpha band PSD, we achieved accurate predictions for 18 out of 21 participants' treatment outcomes, equating to an impressive prediction accuracy of 85.71%. To further assess the robustness of the prediction method with an accuracy of 85.71%, we calculated the sensitivity and specificity. The sensitivity of the devised prediction scheme was found to be 92.8%, indicating the ability to correctly identify non-remission participants, while the specificity was determined to be 71.4%, indicating the capacity to accurately recognize remission participants.

The comparison of the proposed method with other existing approaches is presented in Table IV. Notably, all the methods that demonstrated higher accuracy than the proposed method utilized a larger number of electrodes. Specifically, the proposed method exhibited superior accuracy in predicting treatment non-remission compared to remission while effectively utilizing only one electrode. In comparison to the proposed method, both [15] and [17] yielded lower classification accuracy. Work [16], which employed 16 electrodes, achieved a comparable accuracy to the proposed method. On the other hand, work [18] and [19] which utilizes much higher number of electrodes reported higher classification accuracy.

TABLE IV. COMPARISON OF THE PROPOSED WORK WITH OTHER TREATMENT OUTCOME PREDICTION

Work	Number of participants	Number of electrodes	Accuracy
[15]	51	32	78%
[16]	22	16	87.9%
[17]	10	1	71%
[18]	19	30	96.55%
[19]	19	34	92.28%
Our work	21	1	85.71%

Moreover, [18] employed 10-fold cross-validation, implying that the model was not tested independently for each subject. In the case of [19], the training involved 30 subjects, with only 4 subjects used for testing. As we conducted subject independent LOSO testing, the classification accuracy of the trained model, and consequently, the lower prediction accuracy, may be attributed to the relatively smaller number of participant representations in the remission class. To address this imbalance, we explored techniques such as oversampling the minority class (remission class) features to enhance classification accuracy. However, these efforts did not yield any significant improvements.

One potential scope for future research lies in increasing the number of participants in each treatment arm and including additional measures, such as neuroimaging and clinical features, which could potentially enable the deep learning model to generalize better and yield improved performance. Considering MDD's intricate nature as a complex mood disorder, it is plausible that there may exist subtle EEG signatures that specifically represent non-remission states [27].

VI. CONCLUSION

In this study, we explored the potential of 1DCNNs for predicting treatment remission in MDD following a 10-week home-based treatment trial with active or sham tDCS. The deep learning model of 1DCNNs were trained on pre-treatment EEG data acquired using a portable 4-electrode EEG device. The outputs of the convolutional models were used to make treatment predictions following a proposed prediction rule. To evaluate the effectiveness of various combinations of EEG bands and electrodes, we adopted a subject independent, LOSO testing approach. Our analyses revealed that the PSD vectors extracted from the alpha band and the combination of theta and alpha bands from EEG signals recorded with 4 electrodes, as well as from individual electrodes (e.g., PSD of theta and alpha band combination from TP10 electrode), exhibited higher prediction accuracy, reaching 85.7% accuracy, with sensitivity of 92.8% and specificity of 71.4%. These findings underscored the discriminatory power of certain frequency bands, notably the alpha band and the combination of theta and alpha bands, in differentiating between remission and non-remission states. Furthermore, we conducted an examination of frontal and temporoparietal hemispherical asymmetry's impact on classification accuracy and identified specific electrode pairs contributing to superior results. While the prediction accuracy proved superior for non-remission participants, we acknowledged the potential impact of a smaller number of participants represented in the remission class, which could have influenced the overall performance. Our exploration of oversampling techniques did not yield significant

improvements. The study has several limitations. Primarily, the sample size is modest, encompassing 21 participants, with only 12 undergoing active tDCS treatment and 9 receiving a placebo. Consequently, the outcomes cannot be conclusively attributed to either active tDCS or to sham treatment. Additionally, the EEG data acquisition was limited to four channels, which restricted the spatial resolution. The utilization of portable commercial-grade equipment may not match the potential performance of high-resolution experimental EEG devices. In future research, a larger dataset with an increased number of participants in the remission group could enhance model generalization and overall prediction performance. Given the intricate nature of MDD, it is reasonable to hypothesize that EEG signatures associated with non-remission states may manifest as more distinct than those indicative of remission. Additionally, considering alternative electrode positions that contribute to more discriminative EEGs could be a promising avenue for future research.

In conclusion, our study has demonstrated the potential of one-dimensional CNNs in predicting treatment outcomes to tDCS in MDD based on PSD vectors derived from pre-treatment EEG data. The identification of specific EEG bands and electrodes contributing to higher accuracy provides valuable insights for developing targeted treatment decision-making approaches. Further research and validation with larger datasets are essential to establish the reliability and generalizability of the proposed method for real-world clinical applications [28].

REFERENCES

[1] *Diagnostic and Statistical Manual of Mental Disorders: DSM-5*. Washington, DC: American Psychiatric Publishing, vol. 5, no. 5, 2013

[2] C. D. Mathers and D. Loncar, "Projections of global mortality and burden of disease from 2002 to 2030," *PLoS Medicine*, vol. 3, no. 11, Nov. 2006. doi:10.1371/journal.pmed.0030442

[3] R. C. Kessler *et al.*, "The epidemiology of major depressive disorder," *JAMA*, vol. 289, no. 23, p. 3095, Jun. 2003. doi:10.1001/jama.289.23.3095

[4] C. Roehrig, "Mental disorders top the list of the most costly conditions in the United States: $201 billion," *Health Affairs*, vol. 35, no. 6, pp. 1130–1135, Jun. 2016. doi:10.1377/hlthaff.2015.1659

[5] C. H. Y. Fu, Y. Fan, and C. Davatzikos, "Addressing heterogeneity (and homogeneity) in treatment mechanisms in depression and the potential to develop diagnostic and predictive biomarkers," *NeuroImage: Clinical*, vol. 24, p. 101997, Jan. 2019. doi:10.1016/j.nicl.2019.101997

[6] Practice Guideline for the Treatment of Patients with Major Depressive Disorder. Washington, D.C.: American Psychiatric Association, 2010.

[7] A. S. Widge *et al.*, "Electroencephalographic biomarkers for treatment response prediction in major depressive illness: A meta-analysis," *American Journal of Psychiatry*, vol. 176, no. 1, pp. 44–56, Jan. 2019. doi:10.1176/appi.ajp.2018.17121358

[8] C. Mulert *et al.*, "Rostral anterior cingulate cortex activity in the theta band predicts response to antidepressive medication," *Clinical EEG and Neuroscience*, vol. 38, no. 2, pp. 78–81, Apr. 2007. doi:10.1177/155005940703800209

[9] S. Olbrich and M. Arns, "EEG biomarkers in major depressive disorder: Discriminative power and prediction of treatment response," *International Review of Psychiatry*, vol. 25, no. 5, pp. 604–618, Oct. 2013. doi:10.3109/09540261.2013.816269

[10] V. Knott, C. Mahoney, S. Kennedy, and K. Evans, "Pre-treatment EEG and it's relationship to depression severity and paroxetine treatment outcome," *Pharmacopsychiatry*, vol. 33, no. 6, pp. 201–205, Nov. 2000. doi:10.1055/s-2000-8356

[11] M. Arns, W. H. Drinkenburg, P. B. Fitzgerald, and J. L. Kenemans, "Neurophysiological predictors of non-response to rtms in depression," *Brain Stimulation*, vol. 5, no. 4, pp. 569–576, Oct. 2012. doi:10.1016/j.brs.2011.12.003

[12] M. H. Trivedi *et al.*, "Establishing moderators and biosignatures of antidepressant response in clinical care (EMBARC): Rationale and design," *Journal of Psychiatric Research*, vol. 78, pp. 11–23, Jul. 2016. doi:10.1016/j.jpsychires.2016.03.001

[13] W. Wu *et al.*, "An electroencephalographic signature predicts antidepressant response in major depression," *Nature Biotechnology*, vol. 38, no. 4, pp. 439–447, Apr. 2020. doi:10.1038/s41587-019-0397-3

[14] M. Hamilton, "A rating scale for depression," *Journal of neurology, neurosurgery, and psychiatry*, vol. 23, no. 1, p.56. Feb. 1960

[15] N. Jaworska, S. de la Salle, M.-H. Ibrahim, P. Blier, and V. Knott, "Leveraging machine learning approaches for predicting antidepressant treatment response using electroencephalography (EEG) and Clinical Data," *Frontiers in Psychiatry*, vol. 9, Jan. 2019. doi:10.3389/fpsyt.2018.00768

[16] A. Khodayari-Rostamabad, J. P. Reilly, G. M. Hasey, H. de Bruin, and D. J. MacCrimmon, "A machine learning approach using EEG data to predict response to SSRI treatment for major depressive disorder," *Clinical Neurophysiology*, vol. 124, no. 10, pp. 1975–1985, Oct. 2013. doi:10.1016/j.clinph.2013.04.010

[17] A. M. Al-Kaysi *et al.*, "Predicting tDCS treatment outcomes of patients with major depressive disorder using automated EEG classification," *Journal of Affective Disorders*, vol. 208, pp. 597–603, Jan. 2017. doi:10.1016/j.jad.2016.10.021

[18] M. Sadat Shahabi, A. Shalbaf, and A. Maghsoudi, "Prediction of drug response in major depressive disorder using ensemble of transfer learning with convolutional neural network based on EEG," *Biocybernetics and Biomedical Engineering*, vol. 41, no. 3, pp. 946–959, Jul. 2021. doi:10.1016/j.bbe.2021.06.006

[19] M. Sadat Shahabi, B. Nobakhsh, A. Shalbaf, R. Rostami, and R. Kazemi, "Prediction of treatment outcome for repetitive transcranial magnetic stimulation in major depressive disorder using connectivity measures and ensemble of pre-trained Deep Learning Models," *Biomedical Signal Processing and Control*, vol. 85, p. 104822, Aug. 2023. doi:10.1016/j.bspc.2023.104822

[20] R. D. Woodham, R. M. Rimmer, A. H. Young, and C. H. Y. Fu, "Adjunctive home-based transcranial direct current stimulation treatment for major depression with real-time remote supervision: An open-label, single-arm feasibility study with long term outcomes," *Journal of Psychiatric Research*, vol. 153, pp. 197–205, Sep. 2022. doi:10.1016/j.jpsychires.2022.07.026

[21] R.D. Woodham *et al*., "Home-based transcranial direct current stimulation RCT in major depression," *medRxiv*, Nov. 2023

[22] D.V. Sheehan, *et al*., "The Mini-International Neuropsychiatric Interview (MINI): the development and validation of a structured diagnostic psychiatric interview for DSM-IV and ICD-10," *Journal of clinical psychiatry,* vol. 51, no. 20, pp. 22-33, Jan. 1998

[23] P. Welch, "The use of fast Fourier transform for the estimation of power spectra: A method based on time averaging over short, modified periodograms," in *IEEE Transactions on Audio and Electroacoustics*, vol. 15, no. 2, pp. 70-73, Jun. 1967, doi: 10.1109/TAU.1967.1161901.

[24] S. Hochreiter, J. Schmidhuber, "Long short-term memory," Neural computation, vol. 9, no. 8, pp. 1735-80, Nov. 1997

[25] Cho K, Van Merriënboer B, Gulcehre C, Bahdanau D, Bougares F, Schwenk H, Bengio Y. "Learning phrase representations using RNN encoder-decoder for statistical machine translation," arXiv preprint, arXiv:1406.1078, Jun. 2014

[26] Y. Lecun, L. Bottou, Y. Bengio and P. Haffner, "Gradient-based learning applied to document recognition," in *Proceedings of the IEEE*, vol. 86, no. 11, pp. 2278-2324, Nov. 1998, doi: 10.1109/5.726791

[27] C.H.Y. Fu., M. Antoniades, G. Erus, et al. "Neuroanatomical dimensions in medication-free individuals with major depressive disorder and treatment response to SSRI antidepressant medications or placebo," *Nat. Mental Health*, pp. 164–176 Jan. 2024.

[28] C. H. Fu *et al.*, "Ai-based dimensional neuroimaging system for characterizing heterogeneity in brain structure and function in major depressive disorder: Coordinate-MDD consortium design and Rationale," *BMC Psychiatry*, vol. 23, no. 1, Dec. 2023. doi:10.1186/s12888-022-04509-7